



## Photo-catalytic degradation of Acid Yellow 17 azo dye using ZrO<sub>2</sub>-CeO<sub>2</sub> hollow microspheres as a catalyst

Muhammad Farooq<sup>a,b,\*</sup>, Anita Ramli<sup>b</sup>, Abdul Naeem<sup>a</sup>, Liaqat Ali Shah<sup>c</sup>, Tahira Mahmood<sup>a</sup>, Muhammad Tariq<sup>a</sup>, Jehangeer Khan<sup>a</sup>, Fouzia Perveen<sup>a</sup>, Muhammad Humayun<sup>d</sup>

<sup>a</sup>National Centre of Excellence in Physical Chemistry, University of Peshawar, 25120 Peshawar, Khyber Pakhtunkhwa, Pakistan, Tel. +92 301-8866717; emails: farooq\_khann@yahoo.com (M. Farooq), naeem64@yahoo.com (A. Naeem), tahiramahmood@uop.edu.pk (T. Mahmood), tariq\_ftj@yahoo.com (M. Tariq), jehangeerkhan88@gmail.com (J. Khan), fouziaperveen82@yahoo.com (F. Perveen)

<sup>b</sup>Department of Fundamental and Applied Sciences, Universiti Teknologi PETRONAS (UTP) 31750 Tronoh, Perak, Malaysia, email: anita\_ramli@utp.edu.my

<sup>c</sup>Institute of Process Engineering, Chinese Academy of Sciences, Beijing, China, email: shah@ipe.ac.cn

<sup>d</sup>Department of Basic Sciences, University of Engineering and Technology, Peshawar, Pakistan, email: humayunchemist@uetpeshawar.edu.pk

Received 21 January 2019; Accepted 10 July 2019

### ABSTRACT

In the present study, ZrO<sub>2</sub>-CeO<sub>2</sub> hollow spheres have been synthesized using carbon spheres as a template. The physico-chemical, textural and morphological properties of the synthesized ZrO<sub>2</sub>-CeO<sub>2</sub> hollow spheres were explored by powder X-ray diffraction, N<sub>2</sub>-physisorption, Fourier emission scanning electron microscopy (FESEM) and X-ray photoelectron spectroscopy techniques. The catalytic activity of the synthesized ZrO<sub>2</sub>-CeO<sub>2</sub> catalyst was evaluated in the degradation of acid yellow 17 dye using advanced oxidation technique. The results demonstrated that the ZrO<sub>2</sub>-CeO<sub>2</sub> hollow spheres showed the highest percentage degradation of 88% in reaction time of 180 min for the selected dye. The improved degradation activity of the synthesized catalyst could be attributed to the fact that the oxidizing agent H<sub>2</sub>O<sub>2</sub> react with ZrO<sub>2</sub>-CeO<sub>2</sub> to produce highly reactive hydroxyl radical (\*OH) which further attack on the selected dye molecule and degraded to less environmental toxic components.

**Keywords:** ZrO<sub>2</sub>-CeO<sub>2</sub> hollow spheres; Textural; Morphological properties; Azo dye; Photo-catalytic degradation

### 1. Introduction

Due to rapid industrialization and urbanization, water resources are badly contaminated by different industrial and domestic effluents. The effluents cause serious threat to human society due to their toxic and carcinogenic nature [1–4]. Therefore, remediation of these toxic effluents is one of the triggered challenges worldwide.

Dyes are organic compounds being used in many industries such as textile, leather, paper, printing, cosmetics, petroleum, plastic, food, paint, rubber, and pharmaceutical industries [5–9]. It has been reported that about 146,000

tons organic dyes are introduced into our environment every year [10]. Similarly, the waste water produced from the textile industries containing different dyes is a serious problem all over the world [11]. Dyes and their by-products are highly mutagenic and carcinogenic and when enter the living organisms in excess causes severe health problems. Moreover, the presence of these toxic dyes is potential threat to aquatic life as they may release substances that decrease photo-synthesis process in the plant [12–16]. Second, dyes are very difficult to decolorize using the available techniques due to their complex structure and breakdown nature. Therefore the discharge of such effluents containing different dyes and their breakdown products into the environmental components is critically undesirable [17,18].

\* Corresponding author.

Acid yellow 17 (AY17) is an important commercial azo dye widely used in the textile industries. Azo dyes contain one or more azo groups ( $-N=N-$ ) that have the ability to resist degradation process and therefore accumulate in the environment at high levels with high degree of persistence [19,20]. Although, they are cost effective to produce, but on the other hand, are highly toxic and carcinogenic, causing variety of diseases (such as kidney, bladder and liver cancer).

The discharge of huge amount of these toxic dyes has become a substantial risk to human health and environment [21]. Therefore, appropriate treatment of these refractory organics is very essential to avoid the undesired health and environmental impacts.

Therefore, special efforts are required for the treatment of these toxic pollutants to save the environment. Different technologies such as electrolytic [22], electron beam treatment [23], activated carbon [24,25], photo-catalysis [26] and photo electrochemical [27,28] methods have been employed for the treatment of these toxic effluents.

However, among various methods employed, photo-catalytic or advanced oxidation process has been reported to be very effective, non-expensive and environmental friendly in this regard [29]. Similarly, different metal oxides have been investigated as photo-catalytically active materials for such purposes. Zirconia ( $ZrO_2$ ) is one of the most important functional material in various industries due to its unique properties such as low thermal conduction, high melting point, high strength, high ionic conductivity and chemical inertness [30]. Zirconia is widely used in oxygen sensors, fuel cell electrolytes, catalysts and catalytic supports, metal oxide-semiconductor devices, superior thermal and chemical stability etc. [31–33]. Therefore, several research efforts have been devoted to investigate and improve the structure and properties of the zirconia.

Recently, the hollow zirconia particles have attracted a great deal of attention due to its well-defined morphology, low density, uniform size, large surface area, good permeation and wide range of potential applications, including drug-delivery carriers, nanoscale chemical reactors, catalysis, acoustic insulation, photonic building blocks, development of artificial cells, photonic crystals and so on [34–36]. Likewise, heterogeneous photo-catalysis has gained tremendous attention to be used as the most promising advanced oxidation technology for treatment of various chemical and biological pollutants [37]. In this context, hollow zirconia could be a promising catalyst for the treatment of different effluents by using advanced oxidation technique. Several studies have been made to use metal oxides as a photo-catalyst for the degradation of different dyes. Rani et al. [38] used  $ZrO_2$ /graphene photocatalyst for the removal of Methylene blue (MB) and rhodamine B dyes (RB). However, due to a wide band gap (5.0 eV),  $ZrO_2$  can only be excited for photo-catalysis under UV-light irradiation. Similarly,  $CeO_2$  can also be used as a photo-catalyst for the degradation of dyes and organic pollutants under visible-light irradiation [39]. However, mixing of metal oxide composite materials may further improve the photo-catalytic efficiency by means of increasing the charge separation and extending the visible light absorption. In the previous literature, similar approach of alloying  $ZrO_2$  with  $CeO_3$  has been utilized for improving the photo-catalytic activity of  $ZrO_2$  toward degradation of rhodamine B (RhB) [40,41]. However, several problems

are adhered with the current photo-catalysis technology. Therefore, it is very important to develop an efficient photo-catalyst to counter the problems associated with the advanced oxidation technology for treatment of various chemical and biological pollutants in the near future.

In the present investigation,  $ZrO_2$ - $CeO_2$  hollow spheres have been employed for photo-catalytic oxidation of acid yellow 17 dye as model pollutant to develop an efficient method for treating of toxic effluents. Moreover, the physicochemical properties of the synthesized  $ZrO_2$  hollow spheres were evaluated using different characterization techniques and its reactivity correlated to catalyst properties to develop an efficient catalyst.

## 2. Materials and methods

### 2.1. Reagent

All chemicals used in this study were of analytical grade and used without further purification. Ultra-pure water (resistivity  $\geq 18.2$  M $\Omega$  cm) was used for preparation of standard solutions of Acid Yellow 17. Acid Yellow 17 (Cat. No. 191921000 dye content 60%) was purchased from Acros Organics (Belgium). Hydrogen peroxide ( $H_2O_2$ , 30% w/w),  $ZrOCl_2 \cdot 8H_2O$  (99.0%) and  $Ce(NO_3)_2 \cdot 6H_2O$  (99.0%) were purchased from Sigma-Aldrich (Germany).

### 2.2. Preparation of $ZrO_2$ - $CeO_2$ hollow spheres

Carbon spheres were used as a template to synthesize  $ZrO_2$ - $CeO_2$  solid spheres. Carbon spheres were first synthesized via a hydrothermal reaction as previously reported [36]. About 3.6 g of glucose was first dissolved in 40 mL of distilled water in a flask at room temperature to make a clear solution. The clear glucose solution was then transferred into a Teflon-lined stainless steel autoclave, and was kept at 180°C for 5 h in oven. The autoclave was allowed to cool naturally. The black material so formed was collected, washed with water and absolute ethanol three times, respectively. The carbon spheres were finally dried at 80°C for 5 h.

The carbon spheres were then dispersed in ethanol using ultra-sonication. Required amounts of  $ZrOCl_2 \cdot 8H_2O$  and  $Ce(NO_3)_2 \cdot 6H_2O$  were dissolved in distilled water in two separate beakers to make clear solutions. The salt solutions were first mixed together and then added into dispersed carbon spheres with vigorous stirring. Required amounts of urea and HCl were further added to the carbon sphere mixture to complete the reaction. The mixture was stirred for 10 min and then transferred into autoclave. The autoclave was heated in an oven at 160°C for 24 h. The autoclave was then allowed to cool in the oven. The precipitate was collected carefully and washed three times with water and ethanol, respectively. The collected sample was calcined at 600°C for 5 h in the muffle furnace. The  $ZrO_2$ - $CeO_2$  sample so obtained was stored for further analysis.

### 2.3. Catalytic activity testing in degradation of dye

#### 2.3.1. UV radiation source and photo-Fenton process

Photo-chemical apparatus fitted with a 4 W low pressure Hg-UV lamp (PENRAY, USA) was used for the photo-catalysis

of the selected AY 17 dye in the aqueous solution. The wave length of the light emitted by Hg-UV lamp was 254 nm. The lamp was enclosed in wooden box. A magnetic stirrer was used for stirring the sample to achieve the homogenous flow of UV radiation through the solution. The area of Pyrex glass beaker was 50 cm<sup>2</sup> which was used for sample solution for UV radiation treatment.

### 2.3.2. UV/Vis spectroscopy

Vis spectra were recorded between 300 and 700 nm, employing a double bundled UV/Vis spectrometer (PerkinElmer, Model: Lambda-650, UK) equipped with 1 cm quartz cuvettes. The degradation of AY 17 and the decolorization of the solution were followed by determining the concentration of the remaining dye in the solution. The maximum absorbance wavelength ( $\lambda_{\max}$ ) from the spectra was recorded at 400.0 nm. The highest peak at 400.0 nm was due to absorbance of the  $n-\pi^*$  transition of  $-N=N-$  group in AY 17 molecule. The degraded product does not contain the concentration of AY 17 in entire process [42]. Therefore, the concentration of AY 17 in the reaction mixture was determined at various time intervals by measuring the absorption intensity of the reaction mixture at  $\lambda_{\max} = 400.0$  nm and by using calibration curve. The following equation was used to find the degradation efficiency of the synthesized ZrO<sub>2</sub>-CeO<sub>2</sub> catalyst in AY 17 dye during the photo-catalytic process.

$$\text{Degradation efficiency (\%)} = \frac{(1 - C_t)}{C_0} \times 100 \quad (1)$$

where  $C_0$  is the initial concentration of the AY 17 at  $t = 0.0$  min while  $C_t$  is the concentration of AY 17 at time  $t$  min.

## 3. Results and discussion

### 3.1. BET analysis

N<sub>2</sub> adsorption–desorption analysis was performed to study the textural properties of the synthesized ZrO<sub>2</sub>-CeO<sub>2</sub>

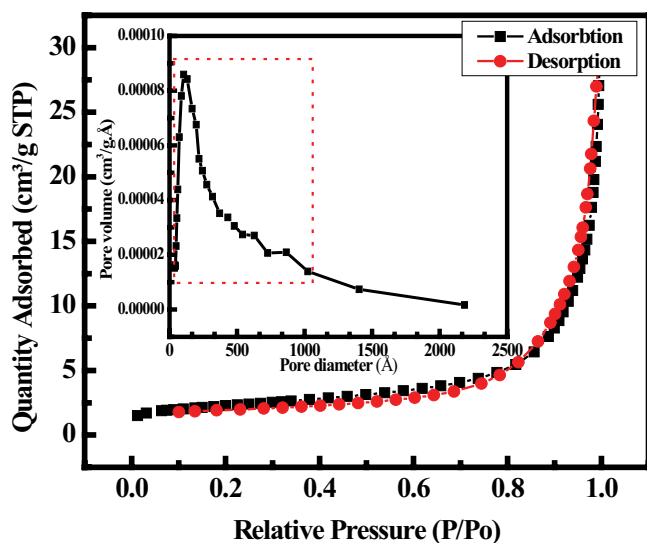


Fig. 1. BET analysis of synthesized ZrO<sub>2</sub>-CeO<sub>2</sub> catalyst.

hollow catalyst and the corresponding data is presented in Fig. 1. The hollow ZrO<sub>2</sub>-CeO<sub>2</sub> catalyst demonstrates high surface area of 202 m<sup>2</sup>/g and average pore width of 164. Moreover, all ZrO<sub>2</sub>-CeO<sub>2</sub> sample displays type IV isotherm with a well-developed type H3 hysteresis loop according to the IUPAC classification [43,44], resulting from the N<sub>2</sub> gas condensation within the clay pots like mesopores.

### 3.2. XRD analysis

The X-ray diffraction (XRD) result of the calcined ZrO<sub>2</sub>-CeO<sub>2</sub> sample along with an un-calcined ZrO<sub>2</sub>-CeO<sub>2</sub> is provided in Fig. 2. It can be seen from the results that the intensities of the peaks increased after calcination of the sample at 600°C. The peaks appeared at 24.38, 28.40, 31.43, 41.48, 50.54, 34.69, 45.75, 55.80 could be attributed to crystalline ZrO<sub>2</sub> particles with monoclinic crystal system as determined from the JCPDS 96-152-2144. The average crystalline size was calculated by the Scherrer formula and was found to be around 8.57 nm. In addition, no clear diffraction peaks corresponding to CeO<sub>2</sub> were observed in the diffraction scans, suggesting that CeO<sub>2</sub> particles were finely dispersed in the ZrO<sub>2</sub> matrix.

### 3.4. XPS analysis

X-ray photoelectron spectroscopy (XPS) analysis was performed to study the oxidation state of cerium and zirconium present in the synthesized ZrO<sub>2</sub>-CeO<sub>2</sub> hollow spheres as shown in Figs. 3 and 4, respectively. It can be seen from Fig. 3 that the Ce 3d spectrum shows three binding energy levels of 884.61, 902.22 and 915.54, which could be assigned to Ce3d 5/2, Ce3d 5/2 and Ce3d 3/2, respectively. Ce3d with binding energy of 884.61 eV has the oxidation state of +3, whereas Ce3d with binding energies of 902.22 and 915.54 eV are referred to the oxidation state of +4. Similarly, the XPS spectrum of zirconium display binding energy levels of

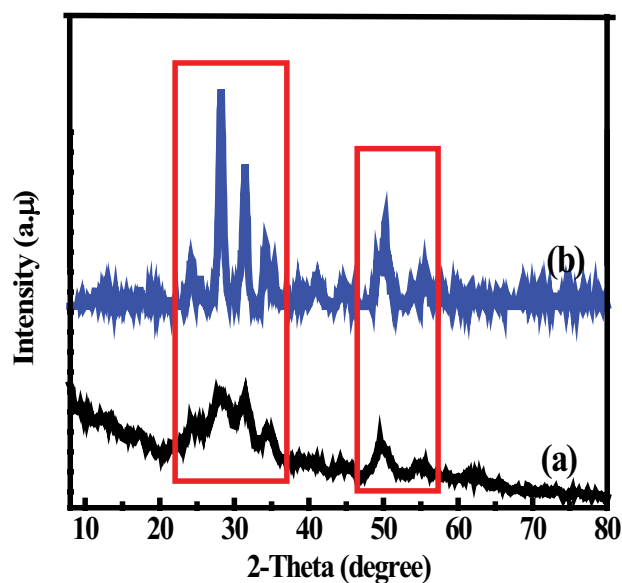


Fig. 2. XRD result of (a) uncalcined ZrO<sub>2</sub>-CeO<sub>2</sub> and (b) calcined ZrO<sub>2</sub>-CeO<sub>2</sub>.

different oxidation states as shown in Fig. 4. The Zr3d binding energies of 182.48 and 184.69 eV are attributed to the oxidation state of +4, whereas the binding energy of 186.91 eV may be assigned to the existence of sub oxidation state of zirconia. The sub oxide form may come in existence due to the argon ion bombardment during the analysis. Further XPS depicts that ZrO<sub>2</sub> is the major oxide present in the ZrO<sub>2</sub>-CeO<sub>2</sub> hollow sphere.

### 3.5. FESEM analysis

The surface morphology and structure of the synthesized hollow ZrO<sub>2</sub>-CeO<sub>2</sub> spheres were studied by field emission scanning electron microscopy coupled with energy-dispersive X-ray analysis (EDX; Fig. 5). FESEM images indicate the hollow spheres of ZrO<sub>2</sub>-CeO<sub>2</sub> with mesoporous structure. The average diameter of hollow ZrO<sub>2</sub>-CeO<sub>2</sub> spheres is about 5.21 μm, and the size of the sphere opening is in the range of 0.84–2.80 μm. The shell thickness was recorded to

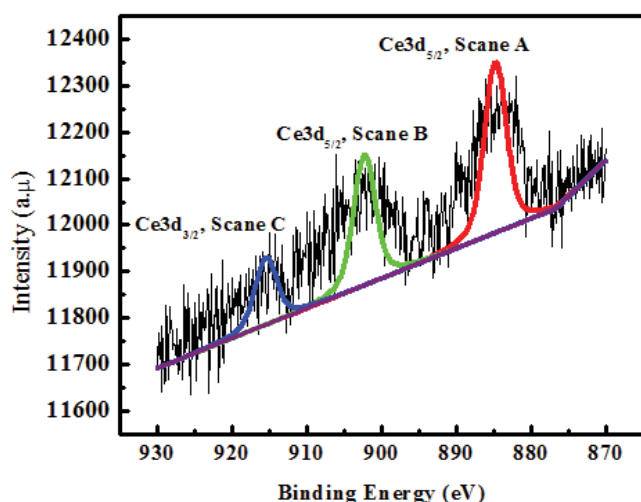


Fig. 3. XPS results of cerium in ZrO<sub>2</sub>-CeO<sub>2</sub>.

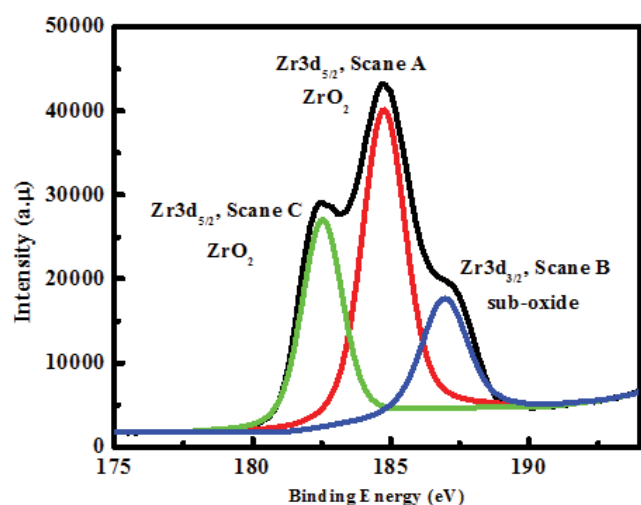


Fig. 4. XPS analysis of zirconium in ZrO<sub>2</sub>-CeO<sub>2</sub>.

be 220 nm. The SEM image further reveals that the spheres are slightly agglomerated and exhibited thick and rough surfaces. The EDX spectrum shows that the synthesized sphere shell includes the desired composition of Zr and Ce elements, showing that ZrO<sub>2</sub>-CeO<sub>2</sub> spheres were successfully prepared using carbon sphere as a template.

### 3.6. Photo-catalytic degradation of Acid Yellow 17 dye

In the present study, the photo-catalytic activity of the synthesized ZrO<sub>2</sub>-CeO<sub>2</sub> porous catalyst toward degradation of the Acid Yellow 17 dye was evaluated. The photo-catalytic activity was determined in terms of percent degradation of the selected dye using the following equation.

$$\text{Degradation (\%)} = \frac{C_0 - C_t}{C_0} \times 100 \quad (2)$$

where  $C_0$  is the initial concentration of AY 17 and  $C_t$  is the concentration of dye at certain interval of time. The percentage degradation of the ZrO<sub>2</sub>-CeO<sub>2</sub> photo-catalyst was found to be 88% in 180 min (Fig. 6). The photo-catalytic degradation activity in AY 17 dye was checked using ZrO<sub>2</sub>-CeO<sub>2</sub> photo-catalyst in the presence of H<sub>2</sub>O<sub>2</sub> (i.e., UV/C/H<sub>2</sub>O<sub>2</sub>) and without H<sub>2</sub>O<sub>2</sub> (i.e., only UV/C). The results were also compared with the homogeneous photo-catalytic system (i.e., UV/H<sub>2</sub>O<sub>2</sub>). It was observed that maximum degradation occurred with UV/C/H<sub>2</sub>O<sub>2</sub>. The absorption spectrum of the AY 17 dye in the presence of UV/C/H<sub>2</sub>O<sub>2</sub> system at pH 3 has been shown in Fig. 7. The absorbance at  $\lambda_{\text{max}}$  (400 nm) decreases with time, which clearly indicates that AY 17 dye efficiently degraded on the surface of ZrO<sub>2</sub>-CeO<sub>2</sub> catalyst

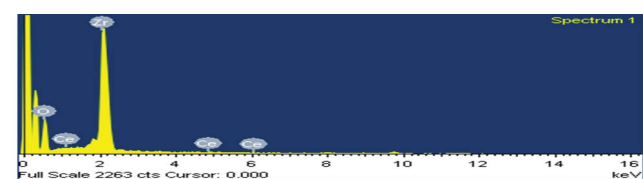
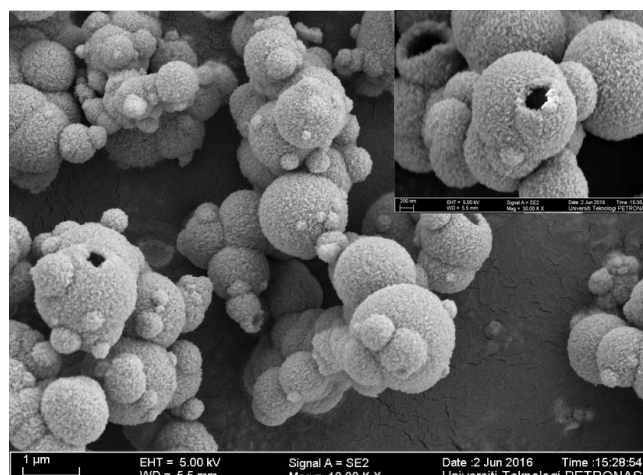
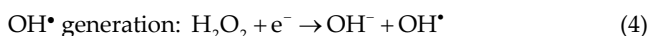
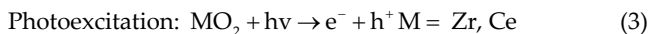


Fig. 5. FESEM coupled with EDX analysis of the ZrO<sub>2</sub>-CeO<sub>2</sub> hollow spheres.

using UV/C/H<sub>2</sub>O<sub>2</sub> system. From these observations, it was inferred that ZrO<sub>2</sub>-CeO<sub>2</sub> photo-catalyst in the presence of H<sub>2</sub>O<sub>2</sub>, promote the generation of highly reactive hydroxyl radical ( $\cdot\text{OH}$ ) which increase the percentage degradation of Acid Yellow 17. The mechanism proposed for photo-catalytic degradation reaction is given by Eqs. (3)–(5) [41].



As the mixing of CeO<sub>2</sub> with ZrO<sub>2</sub> decrease the band gap of the ZrO<sub>2</sub>, the photo-catalytic efficiency increases [40,41].

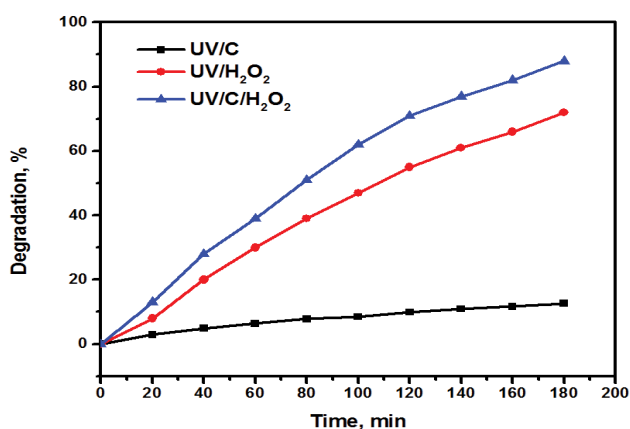


Fig. 6. Effect of various parameters on photo-catalytic degradation of AY 17. Experimental conditions; [AY 17] = 0.14 mM, [H<sub>2</sub>O<sub>2</sub>] = 5 mM, [ZrO<sub>2</sub>-CeO<sub>2</sub>] = 10 mg/L, pH = 3, T = 298 K.

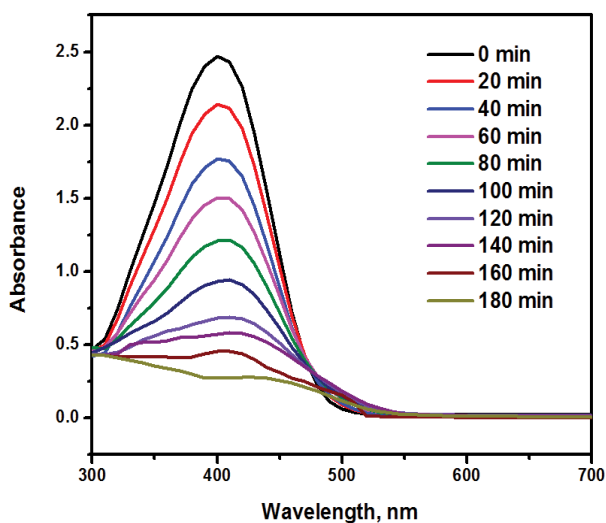


Fig. 7. UV/Vis spectral changes of AY 17 in ZrO<sub>2</sub>-CeO<sub>2</sub> suspensions as a function of time of irradiation. Experimental conditions: [AY 17] = 0.14 mM, [H<sub>2</sub>O<sub>2</sub>] = 5 mM, [ZrO<sub>2</sub>-CeO<sub>2</sub>] = 10 mg/L, pH = 3, T = 298 K.

It was suggested that upon the absorption of photon-energy ( $h\nu$ ) the band-gap of the photo-catalyst becomes equal or exceeds. As a result, the photo-catalytic reaction is initiated with the promotion of photo-excited electron from the filled valence band to the empty conduction band with the generation of electron and hole pair ( $e^-, h^+$ ). Subsequently, the highly reactive hydroxyl radical ( $\cdot\text{OH}$ ) is generated by reaction of photo-excited  $e^-$  with H<sub>2</sub>O<sub>2</sub>, which then attack on the dye molecule. The dye molecule may further decompose through several intermediate steps to the stable products (CO<sub>2</sub> and H<sub>2</sub>O).

### 3.7. Kinetics of photo-catalytic degradation

The kinetics of dye degradation was studied from absorbance data (Fig. 8) using the following integrated Eqs. (6)–(8) [45,46]

$$A_t = A_0 - k_0 t \quad (\text{Zeroth-order}) \quad (6)$$

$$\ln A_t = \ln A_0 - k_1 t \quad (\text{First-order}) \quad (7)$$

$$1/A_t = 1/A_0 + k_2 t \quad (\text{Second-order}) \quad (8)$$

where  $A_0$  is the initial absorbance of the dye,  $A_t$  is the absorbance of the dye solution at any time,  $t$  during degradation.  $A_e$  is the equilibrium absorbance of the dye,  $k_0$ ,  $k_1$  and  $k_2$  are

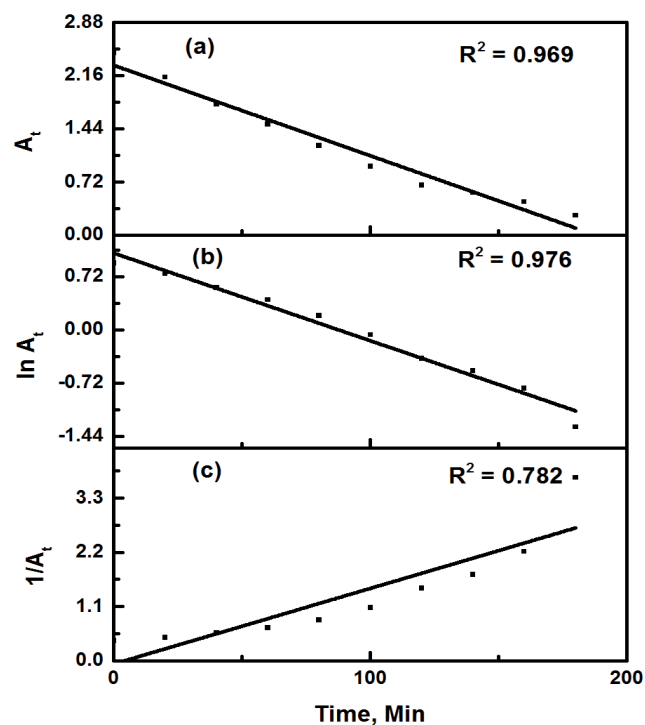


Fig. 8. (a) Plot for zero order kinetic,  $A_t$  vs. time (b) plot for first order kinetic,  $\ln A_t$  vs. time, (c) plot for second order kinetic  $1/A_t$  vs. time. Experimental conditions: [AY 17] = 0.14 mM, [H<sub>2</sub>O<sub>2</sub>] = 5 mM, [ZrO<sub>2</sub>-CeO<sub>2</sub>] = 10 mg/L, pH = 3, T = 298 K.

Table 1  
Kinetic rate constants for degradation of AY 17 by ZrO<sub>2</sub>-CeO<sub>2</sub> porous catalyst

Order of kinetic	Rate constant, $k_n$	$t_{1/2}$ , min	$R^2$
Zero	0.0122 mol L <sup>-1</sup> min <sup>-1</sup>	87.66	0.969
First	0.0118 min <sup>-1</sup>	58.72	0.976
Second	0.0153 mol <sup>-1</sup> L min <sup>-1</sup>	30.55	0.782

the rate constant of zero, first, and second order kinetic equations. The rate constant of the photo-catalytic degradation is depicted in Table 1. From the  $R^2$  it was proposed that the degradation reaction follows first order kinetics.

#### 4. Conclusion

This work describes efficient photo-catalytic degradation of azo dye in the presence of ZrO<sub>2</sub>-CeO<sub>2</sub> hollow catalyst. ZrO<sub>2</sub>-CeO<sub>2</sub> hollow catalyst was successfully prepared by hydrothermal method using carbon spheres as template. The catalyst was further characterized by different analytical techniques. It was noted that ZrO<sub>2</sub>-CeO<sub>2</sub> hollow sphere could be synthesized using carbon spheres. The synthesized catalyst was further tested in dye degradation to develop efficient method for pollutants treatment. It was noticed that the ZrO<sub>2</sub>-CeO<sub>2</sub> hollow spheres carried out 88% dye degradation in reaction time of 180 min. The good performance in the photo-catalytic degradation of the azo dye could be attributed to the production of highly reactive hydroxyl radical (<sup>•</sup>OH) from oxidizing agent H<sub>2</sub>O<sub>2</sub> on the surface of ZrO<sub>2</sub>-CeO<sub>2</sub> catalyst. Hydroxyl radical (<sup>•</sup>OH) group plays an important role in the degradation of the selected dye.

#### References

- [1] K. Saravanakumar, V. Muthuraj, Fabrication of sphere like plasmonic Ag/SnO<sub>2</sub> photocatalyst for the degradation of phenol, *Optik*, 131 (2017) 754–763.
- [2] S.-M. Lam, J.-C. Sin, A.Z. Abdullah, A.R. Mohamed, Degradation of wastewaters containing organic dyes photocatalysed by zinc oxide: a review, *Desal. Wat. Treat.*, 41 (2012) 131–169.
- [3] C. Sahoo, A.K. Gupta, Photocatalytic degradation of methyl blue by silver ion-doped titania: identification of degradation products by GC-MS and IC analysis, *J. Environ. Sci. Health, Part A*, 50 (2015) 1333–1341.
- [4] I.A. Khattab, M.Y. Ghaly, L. Osterlund, M.E.M. Ali, J.Y. Farah, F.M. Zaher, M.I. Badawy, Photocatalytic degradation of azo dye Reactive Red 15 over synthesized titanium and zinc oxides photocatalysts: a comparative study, *Desal. Wat. Treat.*, 48 (2012) 120–129.
- [5] A. Al-Mashaqbeh, B. El-Eswed, R. Banat, F.I. Khalili, Immobilization of organic dyes in geopolymeric cementing material, *Environ. Nanotechnol. Monit. Manage.*, 10 (2018) 351–359.
- [6] S. Chowdhury, R. Mishra, P. Saha, P. Kushwaha, Adsorption thermodynamics, kinetics and isosteric heat of adsorption of malachite green onto chemically modified rice husk, *Desalination*, 265 (2011) 159–168.
- [7] S. Sadaf, H.N. Bhatti, Evaluation of peanut husk as a novel, low cost biosorbent for the removal of Indosol Orange RSN dye from aqueous solutions: batch and fixed bed studies, *Clean Technol. Environ. Policy*, 16 (2014) 527–544.
- [8] H.N. Bhatti, N. Akhtar, N. Saleem, Adsorptive removal of methylene blue by low-cost *Citrus sinensis* bagasse: equilibrium, kinetic and thermodynamic characterization, *Arab. J. Sci. Eng.*, 37 (2012) 9–18.
- [9] K. Sharma Sandeep, H. Bhunia, K. Bajpai Pramod, TiO<sub>2</sub>-assisted photocatalytic degradation of diazo dye reactive red 120: decolorization kinetics and mineralization investigations, *J. Adv. Oxid. Technol.*, 16 (2013) 306–313.
- [10] J. Khan, M. Sayed, F. Ali, M. Khan Hasan, Removal of Acid Yellow 17 Dye by Fenton oxidation process, *Z. Physik. Chemie.*, 232 (2018) 507–525.
- [11] A.F. Martins, M.L. Wilde, C. Da Silveira, Photocatalytic degradation of brilliant red dye and textile wastewater, *J. Environ. Sci. Health, Part A*, 41 (2006) 675–685.
- [12] E. Forgacs, T. Cserhádi, G. Oros, Removal of synthetic dyes from wastewaters: a review, *Environ. Int.*, 30 (2004) 953–971.
- [13] W. Przysaś, E. Zabłocka-Godlewska, E. Grabińska-Sota, Biological removal of azo and triphenylmethane dyes and toxicity of process by-products, *Water Air Soil Pollut.*, 223 (2012) 1581–1592.
- [14] M.A. Hubbe, K.R. Beck, W.G. Neal, Y.C. Sharma, Cellulosic substrates for removal of pollutants from aqueous systems: a review. 2. Dyes, 7 (2012) 96.
- [15] B. Legerská, D. Chmelová, M. Ondrejovič, Decolourization and detoxification of monoazo dyes by laccase from the white-rot fungus *Trametes versicolor*, *J. Biotechnol.*, 285 (2018) 84–90.
- [16] J. Duarte Baumer, A. Valério, S.M.A.G.U. de Souza, G.S. Erzinger, A. Furigo, A.A.U. de Souza, Toxicity of enzymatically decolorized textile dyes solution by horseradish peroxidase, *J. Hazard. Mater.*, 360 (2018) 82–88.
- [17] C. Zaharia, D. Suteu, A. Muresan, R. Muresan, A. Popescu, Textile wastewater treatment by homogenous oxidation with hydrogen peroxide, *Environ. Eng. Manage. J.*, 8 (2009) 1359–1369.
- [18] B. Krishnakumar, R. Hariharan, V. Pandiyan, A. Aguiar, A.J.F.N. Sobral, Gelatin-assisted g-TiO<sub>2</sub>/BiOI heterostructure nanocomposites for azo dye degradation under visible light, *J. Environ. Chem. Eng.*, 6 (2018) 4282–4288.
- [19] P. Saranraj, V. Sumathi, D. Reetha, D. Stella, Decolourization and degradation of direct azo dyes and biodegradation of textile dye effluent by using bacteria isolated from textile dye effluent, *J. Ecobiotechnol.*, 2 (2010) 7–11.
- [20] T. Agarwal, R. Singh, Bioremediation potentials of a moderately halophilic soil bacterium, *J. Pharm. Biomed. Sci.*, 19 (2012) 1–6.
- [21] F.M.D. Chequer, G.A.R. de Oliveira, E.R.A. Ferraz, J.C. Cardoso, M.V.B. Zanoni, D.P. de Oliveira, Textile Dyes: Dyeing Process and Environmental Impact. Eco-friendly Textile Dyeing and Finishing, InTech, 2013.
- [22] M.A. Jorquera, G. Valencia, M. Eguchi, M. Katayose, C. Riquelme, Disinfection of seawater for hatchery aquaculture systems using electrolytic water treatment, *Aquaculture*, 207 (2002) 213–224.
- [23] H.-S. Shin, Y.-R. Kim, B. Han, I.E. Makarov, A.V. Ponomarev, A.K. Pikaev, Application of electron beam to treatment of wastewater from papermill, *Radiat. Phys. Chem.*, 65 (2002) 539–547.
- [24] L.-L. Hwang, J.-C. Chen, M.-Y. Wey, The properties and filtration efficiency of activated carbon polymer composite membranes for the removal of humic acid, *Desalination*, 313 (2013) 166–175.
- [25] M. Inyang, B. Gao, L. Wu, Y. Yao, M. Zhang, L. Liu, Filtration of engineered nanoparticles in carbon-based fixed bed columns, *Chem. Eng. J.*, 220 (2013) 221–227.
- [26] A. Mehta, A. Mishra, M. Sharma, S. Singh, S. Basu, Effect of silica/titania ratio on enhanced photooxidation of industrial hazardous materials by microwave treated mesoporous SBA-15/TiO<sub>2</sub> nanocomposites, *J. Nanopart. Res.*, 18 (2016) 209.
- [27] L. Liu, G. Zhang, J.T. Irvine, Y. Wu, Organic semiconductor g-C<sub>3</sub>N<sub>4</sub> modified TiO<sub>2</sub> nanotube arrays for enhanced photoelectrochemical performance in wastewater treatment, *Energy Technol.*, 3 (2015) 982–988.
- [28] T.-C. An, X.-H. Zhu, Y. Xiong, Feasibility study of photoelectrochemical degradation of methylene blue with three-dimensional electrode-photocatalytic reactor, *Chemosphere*, 46 (2002) 897–903.

- [29] T. Ben-Moshe, I. Dror, B. Berkowitz, Copper oxide nanoparticle-coated quartz sand as a catalyst for degradation of an organic dye in water, *Water Air Soil Pollut.*, 223 (2012) 3105–3115.
- [30] Z. Shu, X. Jiao, D. Chen, Template-free solvothermal synthesis of size-controlled yttria-stabilized-zirconia hollow spheres, *J. Alloys Comp.*, 509 (2011) 9200–9206.
- [31] G. Ćirić-Marjanović, Recent advances in polyaniline research: polymerization mechanisms, structural aspects, properties and applications, *Synth. Metals*, 177 (2013) 1–47.
- [32] A. Khan, A.A.P. Khan, A.M. Asiri, V. Gupta, M. Rathore, Preparation, properties and applications of organic-inorganic hybrid nanocomposite poly(aniline-co-o-toluidine) tungstomolybdate, *J. Mol. Liq.*, 216 (2016) 646–653.
- [33] S.-X. Wang, Z.-C. Tan, Y.-S. Li, L.-X. Sun, Y. Li, A kinetic analysis of thermal decomposition of polyaniline/ZrO<sub>2</sub> composite, *J. Thermal Anal. Calorim.*, 92 (2008) 483–487.
- [34] R. Chen, J. Yu, W. Xiao, Hierarchically porous MnO<sub>2</sub> microspheres with enhanced adsorption performance, *J. Mater. Chem. A*, 1 (2013) 11682–11690.
- [35] J. Hu, M. Chen, X. Fang, L. Wu, Fabrication and application of inorganic hollow spheres, *Chem. Soc. Rev.*, 40 (2011) 5472–5491.
- [36] C. Wang, Y. Le, B. Cheng, Fabrication of porous ZrO<sub>2</sub> hollow sphere and its adsorption performance to Congo red in water. *Ceramics Int.*, 40 (2014) 10847–10856.
- [37] A. Fujishima, X. Zhang, D.A. Tryk, TiO<sub>2</sub> photocatalysis and related surface phenomena, *Surf. Sci. Rep.*, 63 (2008) 515–882.
- [38] S. Rani, M. Aggarwal, M. Kumar, S. Sharma, D. Kumar, Removal of methylene blue and rhodamine B from water by zirconium oxide/graphene, *Water Sci.*, 30 (2016) 51–60.
- [39] D. Channei, B. Inceesungvorn, N. Wetchakun, S. Ukritnukun, A. Nattestad, J. Chen, S. Phanichphant, Photocatalytic degradation of methyl orange by CeO<sub>2</sub> and Fe-doped CeO<sub>2</sub> films under visible light irradiation, *Sci. Rep.*, 4 (2014) 5757.
- [40] X. Wang, B. Zhai, M. Yang, W. Han, X. Shao, ZrO<sub>2</sub>/CeO<sub>2</sub> nanocomposite: two step synthesis, microstructure, and visible-light photocatalytic activity, *Mater. Lett.*, 112 (2013) 90–93.
- [41] M. Li, S. Zhang, L. Lv, M. Wang, W. Zhang, B. Pan, A thermally stable mesoporous ZrO<sub>2</sub>-CeO<sub>2</sub>-TiO<sub>2</sub> visible light photocatalyst, *Chem. Eng. J.*, 229 (2013) 118–125.
- [42] K.S.W. Sing, D.H. Everett, R.A.W. Haul, L. Moscou, R.A. Pierotti, J. Rouqu  rol, T. Siemieniewska, Reporting physisorption data for gas/solid systems with special reference to the determination of surface area and porosity (Recommendations 1984), *Pure Appl. Chem.*, 57 (1985) 603–619.
- [43] J. Li, Z. Song, P. Ning, Q. Zhang, X. Liu, H. Li, Z. Huang, Influence of calcination temperature on selective catalytic reduction of NO<sub>x</sub> with NH<sub>3</sub> over CeO<sub>2</sub>-ZrO<sub>2</sub>-WO<sub>3</sub> catalyst, *J. Rare Earths*, 33 (2015) 726–735.
- [44] M. Moradi, F. Ghanbari, M. Manshouri, K.A. Angali, Photocatalytic degradation of azo dye using nano-ZrO<sub>2</sub>/UV/persulfate: response surface modeling and optimization, *Korean J. Chem. Eng.*, 33 (2016) 539–546.
- [45] S.-P. Sun, C.-J. Li, J.-H. Sun, S.-H. Shi, M.-H. Fan, Q. Zhou, Decolorization of an azo dye Orange G in aqueous solution by Fenton oxidation process: effect of system parameters and kinetic study, *J. Hazard. Mater.*, 161 (2009) 1052–1057.
- [46] M. Karatas, Y.A. Argun, M.E. Argun, Decolorization of anthraquinonic dye, Reactive Blue 114 from synthetic wastewater by Fenton process: kinetics and thermodynamics, *J. Ind. Eng. Chem.*, 18 (2012) 1058–1062.